The colours of the ocean plastics

Elisa Martí[1*], Cecilia Martin[2], Matteo Galli[3], Fidel Echevarría[1], Carlos M. Duarte[2], Andrés Cózar[1*]

[1] Departamento de Biología, Campus de Excelencia Internacional del Mar (CEIMAR), Instituto Universitario de Investigaciones Marinas (INMAR), Universidad de Cádiz, E-11510 Puerto Real, Spain

[2] King Abdullah University of Science and Technology, Red Sea Research Center, Thuwal 23955-6900, Kingdom of Saudi Arabia

[3] Department of Physical Sciences, Earth and Environment, University of Siena, Via P.A. Mattioli 4, 53100, Siena, Italy

* Corresponding authors: elisa.marti@uca.es; andres.cozar@uca.es

Abstract

Characterisation of the colour is often included in studies on plastic pollution. However, the comparability and relevance of this information is limited by methodology or observer subjectivity. Based on the analysis of thousands of floating plastic fragments from a global collection, here we propose a systematic semi-automatic method to analyse colours by using a reference palette of 120 Pantone colours. The most abundant colours were white and transparent/translucent (47 %), yellow and brown (26 %) and blue-like (9 %). The white colour increased in the smallest pieces (< 5 mm) and far from coastal sources (> 500 km). Both fragmentation and discolouration of ocean plastics may occur because of longer exposure time to sunlight in nature. In addition, yellow items peaked at around 1 cm and brown colours at around 1 mm, supporting the notion that yellowing precedes tanning in the aging process, which is paralleled by fragmentation. Apart from the effects of the weathering, our results suggest a second-order modulation of the colour distributions of marine plastic microplastics by the selective action of visual predators. The present work provides methodological tools and a wide empirical background to further the interpretation and applicability of the colour information on ocean plastics.

Table of Contents (TOC) Art

Introduction

Plastic pollution spreads throughout the global ocean (Cózar et al. 2014; Eriksen et al. 2014; van Sebille et al. 2015). The weathering of plastic debris in the environment leads to a progressive degradation of the chemical bond structure of the polymers (Brandon et al. 2016; ter Halle et al. 2017). Despite this degradation, plastics hardly disappear in nature. Plastic objects break down into smaller and smaller pieces, which are transported by currents across the oceans to reach even the most remote areas (Zhang 2017; Cózar et al. 2017).

We have a limited knowledge about the transformation of the plastic debris in the environment. The stages of weathering or the time scales of degradation, fragmentation and transport in the marine environment are poorly understood. While staying in inland environments, stranding on the shores or floating at the ocean surface, plastic debris undergoes photo-oxidation and changes in the absorbance and reflection of light, acquiring scratched surface and shifts in its tonality (Weinstein et al. 2016; ter Halle et al. 2016; Brandon et al. 2016). Due to weathering, discolouration (Pospísil et al. 2002) and the development of yellowish colours are common features on plastics aged in the environment (Andrady et al. 1992; Singh et al. 2001; Yousif & Haddad 2013; Pastorelli et al. 2014). Thus, the size as well as the colour of oceanic plastic debris may reflect their degradation stages and be potentially used as proxies of exposure time in the environment.

Numerous studies have accounted for the plastic colour, using from simple sorting with 4 colour categories (Shaw & Day 1994; Barrows et al. 2017) to more detailed classifications based on up to 32 colours (Blair Crawford & Quinn 2017). There is a pressing demand for replicable and objective methods to analyse the colour of ocean

plastic (Hartmann et al. 2019). However, standard procedures for colour categorisation are lacking thus far. At present, the process of categorisation of colours is highly subjective and depends, among others, on visual capabilities and experience of observer. The lack of standardized methods imposes significant difficulties to compare studies and achieve robust conclusions.

In the present work, we characterized the colour of thousands of items collected with surface trawling plankton nets at the global scale. Our main goal is to use this extensive analysis to define a consistent methodological tool to characterize colour in marine plastic samples. Additionally, we provide a robust benchmark against which future data sets can be compared to and explore potential insights the colour information may offer on sources and fate of marine plastics. Based on weathering experiments (Andrady 2017), we expect photo-oxidative damage to lead to increasing fractions of white and yellow-brown colours in ocean plastics with increasing exposure time in the environment, parallel to reduction in their sizes (ter Halle et al. 2017). Likewise, the transport of plastic fragments to distant open-ocean accumulations is proposed to be a time-dependent process, with the fragments far from shore being, on average, older than nearby ones (Brandon et al. 2016). Here we explore the relationships between colours of marine plastic debris with particle size and distance to the coast. These relationships may, in turn, support the use of colour information to provide insights onto the nature and dynamics of marine plastic litter.

Material and Methods

Marine plastic items were collected by surface trawling nets in the circumnavigation cruise “Malaspina 2010” together with other regional surveys carried out from 2010 to 2017 (Table 1). Samplings covered open-ocean plastic accumulation zones located in

each of the five sub-tropical gyres (North Pacific, North Atlantic, South Pacific, South Atlantic and Indian Ocean) as well as semi-enclosed regions (Mediterranean, Arctic Ocean, Red Sea and Bay of Biscay). Overall, 8,849 items with sizes from 0.2 mm to 15 cm were collected from surface waters with distance to land ranging from 0.2 to 3,000 km (Fig. S1). Distances were measured to the nearest continental coasts, excluding the coasts of small oceanic islands. Regarding the polymeric composition of the plastic items, a previous work carried out on a subset of 694 items showed that 94.2 % of the fragments were made of polyethylene (PE) and polypropylene (PP) (Serranti et al. 2018). Other major commodity plastics such as polystyrene (PS), polyethylene terephthalate (PET) or polyvinyl chloride (PVC) were barely represented in the dataset.

Table 1. Summary of sampling regions, date and number of plastic items (N = 8,849) collected using surface trawling nets. Location of sampling sites is shown in Figure S1.

Region/Cruise	Date	No. Items	Ref.
Malaspina Circumnavigation and others	2010 - 2011	2994	Cózar et al. 2014
Mediterranean Sea	2013	3369	Cózar et al. 2015
Arctic Ocean	2013	775	Cózar et al. 2017
Red Sea	2016 - 2017	297	Martí et al. 2017
Atlantic Ocean	2015	452	This study
Strait of Gibraltar	2015	525	This study
Bay of Biscay	2017	437	This study

Colour of all plastic items was categorized using a reference palette with 13 main colours and 9 hues from black to white, besides the transparent/translucent, accounting for a total of 120 possible colour codes (120-Palette, Fig. 1; see Table S1 for RGB

scores and Pantone´s codes). Based on the experience acquired during the analyses, we selected a 120-colours scheme in order to find a balanced equilibrium between analytical effort and level of detail provided by the results. Human capacity to assign colours may vary between observers since it depends on the particular features of the observer´s retina and prior experience. By using a reference palette, here we aim to minimize differences in the observer´s capacity to assign colours. Two alternatives are proposed to the palette-assisted assignment of colours, a visual method and a digital semi-automatic method, both providing comparable results (see Supporting Methods). Both methods are applied once the plastics were washed and dried. The reflectance of wet and dry plastic is different, leading to more stable data from dry samples. Therefore, all plastic pieces were washed with ultrapure water and analysed once they were completely dry in order to render the results comparable and the analyses reproducible.

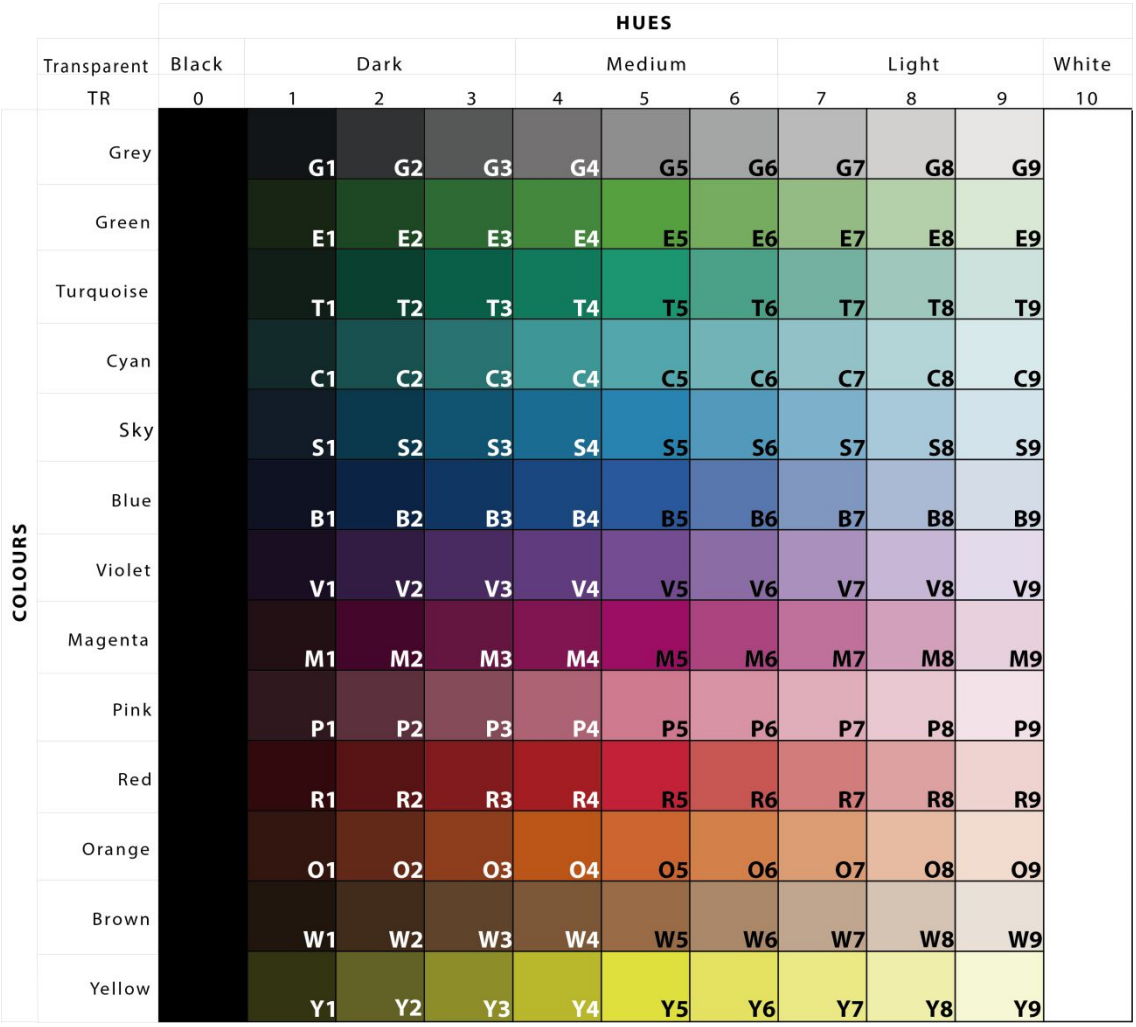

Figure 1. Palette of 120 colour codes (120-Palette) that includes 13 colours (vertical axis) and 9 hues (horizontal axis) from black to white, besides the transparent/translucent. RGB scores and Pantone´s codes are shown in Table S1. A simplified version of this reference palette can be derived from the aggregation of dark, medium and light hues (42-Palette, see Methods).

Visual palette-assisted method for colour assignment

Dried plastic items were organized into glass Petri dishes by main colours. The printed colour palette was placed under the Petri dish as reference and colour codes were assigned to the items by visual similarity (Fig. S2). To ensure the replicability of the

printed version of the 120-Palette, we also provide Pantone´s codes for all colours in the reference palette (Table S1). When the colour of an item was markedly heterogeneous, for instance due to biofouling, an additional secondary colour was registered. A low percentage of double colour assignment was needed (< 2 % of the total), and finally the analyses were exclusively based on the primary colour.

Digital semi-automatic method for colour assignment

From the experience acquired here, we developed a digital method for colour assignment to facilitate future analyses. A subsample of plastic items (N = 103) was processed by the digital method for comparative purposes. Dry plastic items were photographed with a high-resolution camera (NIKON D810, exposure 1/15 sec, aperture f/4.5 and no flash) and examined using ImageJ (https://imagej.nih.gov/ij/). This software, like other common image analysers, provides a digital colour categorization through a combination of scores for red, green and blue colours (RGB) on a 0 to 255 scale. Thus, RGB palette comprises 16,777,216 colours (256^3). To convert any RGB score into one of the 120 colours in the reference palette, RGB scores for each of the colour codes from the 120-Palette were used as reference nodes in the three-dimensional RGB colour space (Table S1; Fig. S3). Therefore, by identifying the reference node at the minimum distance from the RGB scores of a given item, one of the 120 colours of the reference palette may be automatically assigned to any RGB score by proximity in the colour space (see Supporting Methods).

Size and shape of the plastic items

The size of the plastics was measured from the high-resolution photographs using ImageJ software. Items were also classified according to shape/origin in six types: raw industrial pellets, microbeads (likely derived from cosmetic and cleansing products),

films (mostly derived from discarded bags and wrappings), foamed plastic, rigid (thick-walled) fragments, and fishing lines (likely also derived from nets). The colour pattern for each plastic type was examined using principal components analysis (PCA) from the SPSS statistical package (version 24). Due to the low representation of some colours, we used a simplified version of the reference palette for the PCA (36-Palette). This version grouped in dark (hues 1, 2 y 3, Fig. 1), medium (hues 4, 5 y 6) and light (hues 7, 8 and 9), and grouped violet, magenta and pink (which represented only 0.88 % in our dataset) as wide magenta.

Possible trends in the colour spectra were examined in relation to plastic size and distance to the coast, explored here as potential proxies of the age of plastic litter in the marine environment (Brandon et al. 2016; ter Halle et al. 2017). A Single Value Decomposition (SVD) was used to infer which colours showed similar covariance with size or distance to land. SVD provides a series of eigenfunctions associated with dominant modes of colour variability. For each eigenfunction, the related eigenvalue indicates the fraction of the total variability explained. Significant eigenfunctions were then compared to the variability patterns of the percentage of each colour in relation to size or distance to nearest continental coast. Using the Pearson correlation coefficient, the colour codes were linked to the main eigenfunctions and gathered into groups having similar co-variation. Colours that were not significantly related to any of the main eigenfunctions were represented jointly as “Rest of colours”.

Results

As a first step, the colour spectrum of the complete collection of plastic items (n = 8,849) was analysed by using the visual method assisted with the reference palette of 120 colour codes (120-Palette). We found a wide range of colours (103 of the 120 used

157 in the palette), with a prevalence of white, transparent/translucent, black, blue-like and
158 yellow-brown colours. Rigid (thick-walled) fragments were the most abundant plastic
159 type, accounting for 84 % of the total items analysed (Table S2). Rigid fragments also
160 showed the widest colour diversity. Film-type plastics were mainly related to
161 transparent/translucent items, while fishing lines were highly related to blue, turquoise
162 and green colours (Fig. 2, Fig. S6).

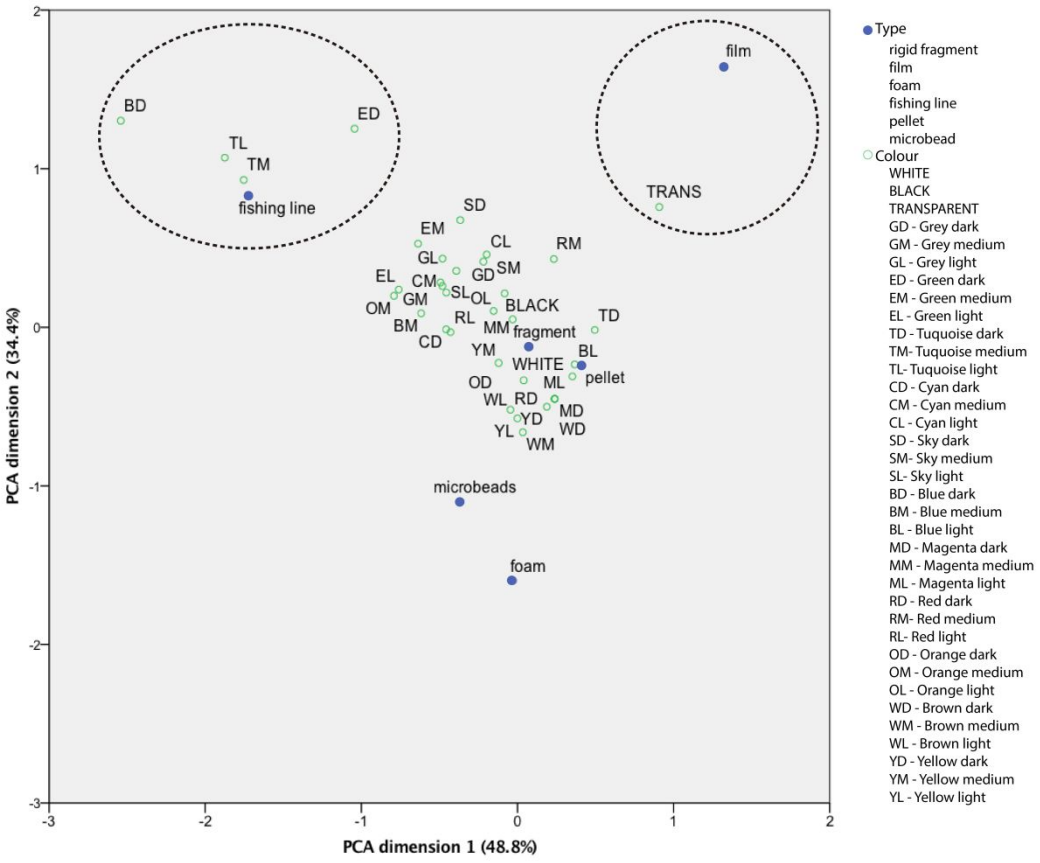

163

164 **Figure 2.** Biplot for the PCA analysis of plastic type and colour. All items (N = 8,849)
165 are plotted in relation to the first two principal components, accounting for 83.2 % of
166 the variability ($\chi 2$ = 1,892, df = 175, $p < 0.05$). Fishing lines were located in the upper
167 left, related to BD, TL, TM and ED colours (see left legend). Films were located in the
168 upper right, being mainly transparent/translucent (TRANS). Data used for this figure are
169 provided in Table S2 and graphed in bar charts in Fig. S6.

Our analyses focused on the colour-hue matrix for rigid fragments since this plastic type was by far the most abundant in the samples. Apart from white, transparent/translucent and black, which were particularly common (31 %, 16 % and 7 % of the total, respectively), there were three zones in the matrix showing high abundance of items (Fig. 3). Amber colours, that is, those in the range of yellow-brown-orange, added a 28 % of the total items, bluish-green colours encompassed an 11 %, and grey colours accounted for a 5 %. The lowest proportion was detected in reddish tonalities (violet, magenta, pink and red), which gathered just a 2 % of the total of rigid fragments. Projecting data on the hue axis of the matrix (Fig. 3), we found maxima at yellow and brown colours and an increasing trend in abundance towards the lightest hues.

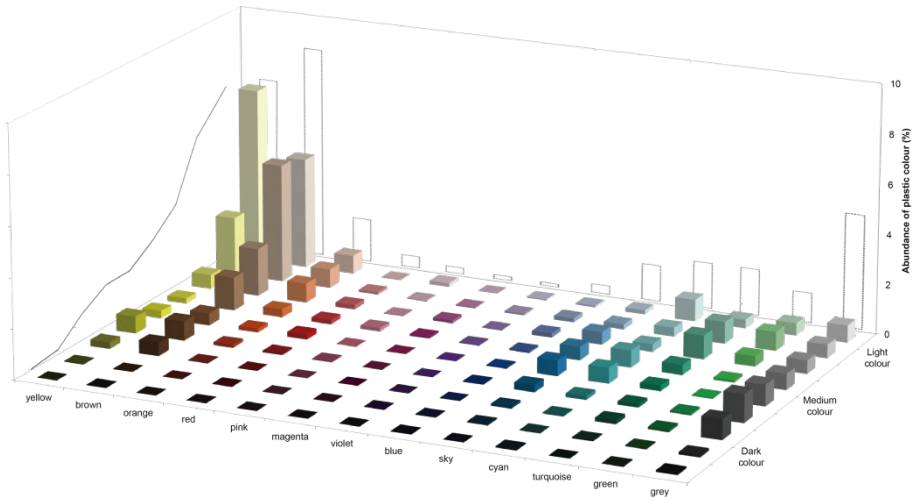

Figure 3. Proportions of colour for rigid plastic fragments (n = 7,395) in the 120-Palette. Percentages of hues and colours are added and projected on left and back planes, respectively, showing increasing percentages towards the lightest hues and maxima at yellow and brown colours. Note that the graph excludes white, transparent/translucent and black (31 %, 16 % and 7 %, respectively). Colour

189 assignment was carried out by the visual palette-assisted method. Numerical
190 percentages for each colour are provided in Table S3.

191

192 The covariance of colours in relation to distance to land and plastic size was determined
193 through SVDs using only rigid fragments for the analysis (Fig. 4). In terms of distance
194 to land, the four main principal components explained 93 % of the colour variability.
195 PC1 was related to the variability of white and light-cyan colours. The abundance of
196 these colours was around 15 % near the shores and rapidly increased from 500 km to
197 coast, accounting for 70 % of all items at distances larger than 2,000 km (Fig. 4A). The
198 offshore increase in the proportion of white and light-cyan was not observable just from
199 the semienclosed-seas dataset (Mediterranean and Red Sea, Fig. S7), likely because all
200 these sampling sites were located relatively close to land (< 500 km). Likewise, the
201 group of "Rest of colours" was mostly represented by medium colour tonality in the
202 semi-enclosed seas (53 %) while light colour tonality was predominant into this group
203 in the open-ocean dataset (55 %). "Rest of colours" showed an increasing trend
204 landward, contrary to the white colour.

205 Four components explained 82 % of the variability of colours in relation to the plastic
206 size gradient (Fig. 4B). White colour predominated throughout the whole size gradient,
207 especially in the open-ocean dataset (Fig S8), which accounted for more distant zones
208 from land. An increasing trend in the proportion of white items towards small sizes was
209 found in the joint dataset, particularly from 0.5 to 5 millimeter in size. Interestingly, the
210 proportion of yellow colours showed maxima around 10 mm in size, while brown
211 colours peaked around 1 mm. Moreover, yellow and brown colours showed similar

patterns in both datasets, open ocean and semi-enclosed seas, in spite of the differences in the load of white fragments.

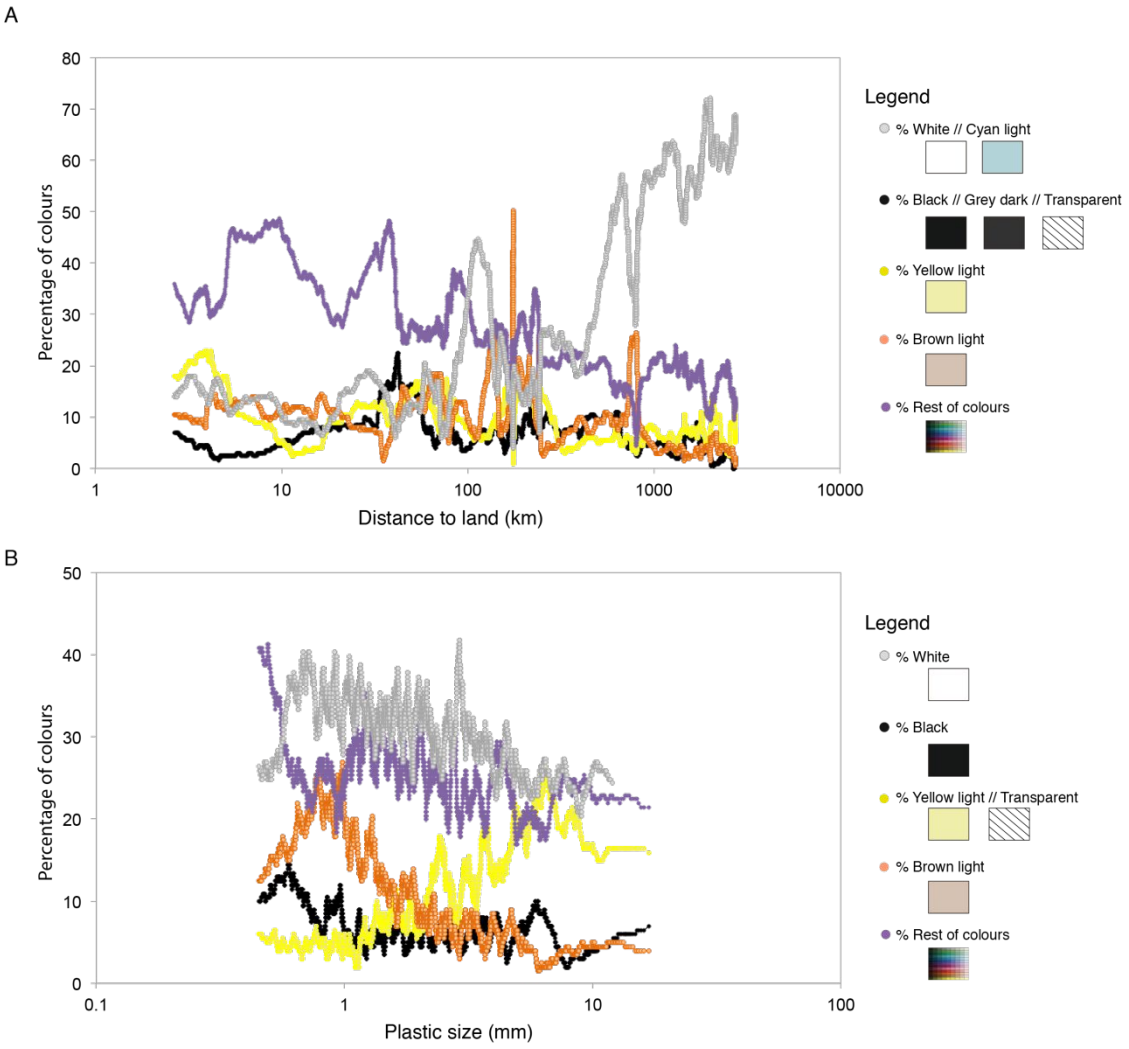

Figure 4. Percentages of colour in relation to distance to land (A) and plastic size (B). Percentages were calculated for moving averages of 200 rigid plastic fragments. Single Value Decomposition (SVD) and Pearson correlation coefficients were used to group colours showing similar covariance in relation to distance to land and size. Figure legends show the main colour groups. "Rest of colours" was dominated by bluish colours (cyan, sky and blue, > 22 %) in B, while it comprised a higher diversity of colours in A. Colour assignment was carried out by the visual palette-assisted method.

Discussion

The present study provides the most exhaustive and comprehensive analysis of the colour of marine plastic debris. A total of 8,849 floating items collected from around the world were classified by using a 120-colour palette, accounting for differences in plastic typology, size and distance to land. Rigid fragment was the most abundant plastic type (84 % of the total items), in agreement with observations of other authors in oceanic surface waters (Morét-Ferguson et al. 2010; Reisser et al. 2015). Therefore, the analyses of colour patterns in relation to particle size and distance to land focused on the collection of rigid fragments in order to avoid confounding effects of changes in plastic types on colour distributions (Fig. 2).

Photo-oxidation is a known process that induces changes in both mechanical properties and colour of the plastic polymers. Comparing recently-manufactured objects, mesoplastic pieces (5 - 20 mm) and microplastics (0.3 - 5 mm), ter Halle et al. (2017) found a progressive oxidative degradation of the polymers, with evident changes in properties such as crystallinity and molar mass towards smaller plastic sizes. Oxidative degradation of plastics during weathering determines the ease of crack formation and fragmentation. In parallel, photo-oxidation generally causes changes in plastic colour, with experimental weathering tests leading to the expectation of gradual change towards light colours (discolouration or whitening), while the accumulation of degradation products in the plastic matrix as result of the oxidation typically gives yellow or amber colours (yellowing and tanning, respectively) (Andrady 2017).

Open-ocean samples comprised a considerably high fraction of white items (26 %), much higher than those in semi-enclosed seas (6 %). The proportion of white items increased from 15 % to 70 % beyond 500 km from land (Fig. 4A), supporting the

hypothesis of progressive discolouration as plastic debris moves away offshore. Based on the changes in the chemical bonds of polyethylene particles, Brandon et al. (2016) inferred exposure times longer than 18 months for floating particles collected far from shores, into the accumulation zone of the North Pacific Central Gyre, while particles sampled in both intermediate and near-shore waters could have generally weathered less than 18 months. The relationship between white items and particle size showed the highest proportions of white particles in the microplastic size range, from 0.5 to 5 mm (Fig. 4B). This pattern was particularly evident in the open-ocean dataset (Fig. S8), likely because the semi-enclosed dataset was biased towards samples collected at relatively short distances from the coast (< 500 km to land) and its load of white items was relatively low.

Like white items, the fraction of light-cyan items also increased far from shore (Fig. 4A). Light-cyan colour may be derived from the discolouration of bluish colours. Indeed, we found a considerable number of bluish items (cyan, sky and blue), contrasting with the very low number of reddish items (violet, magenta, pink and red) (Fig. 3). Interestingly, Shaw and Day (1994) found similar colour-dependent loss of floating microplastics in the North Pacific Ocean. A possible explanation could be related to a lower removal of bluish plastics from the ocean surface by plastic-ingesting predators such as seabirds or vertically migratory fish, as suggested by Shaw and Day (1994). Blue has been suggested as a common camouflage colour in the ocean surface (Hudelson 2011; Umbers 2012). Thus, blue pigmentation is commonly used for the organisms living on the surface, with successful blue-coloured life forms in the neuston such as *Velella velella*, *Porpita porpita*, *Glaucus atlanticus* or many species of oceanic copepods (Fig. S9). A higher probability of detection and ingestion of items with non-blue colours, like red coloured, by visual surface predators would lead to a progressive

enrichment in blue microplastics on the ocean surface. In lakes without zooplanktivorous pressure, a more cost-effective red pigmentation is used by the zooplankton to protect themselves against UV radiation; however, UV-protective pigment is turned from red to blue in order to reduce the losses by predation when zooplanktivorous fishes increase (Hudelson 2011). Therefore, if the removal of microplastics from the surface by visual predators becomes a significant sink process in the open ocean, we could expect an increase in the proportion of blue-like colours, especially towards the smallest sizes, as observed (Shaw & Day 1994), because the effect on the colour distribution would be cumulative. However, we note that some visual predators have been shown to have preferential ingestion for blue prey, as in the case of small planktivorous fishes along the coast of Easter Island, in the South Pacific Subtropical Gyre. Ory et al. (2017) found that these fishes regularly ingest blue plastic fragments that resemble their common prey items, blue copepods. A second possible explanation for the increase of light cyan items towards remote areas and among the smallest items could be that the fragmentation of fishing lines, abundant in bluish colours (Fig. 2, Fig. S6) is generating small pieces not identifiable as fishing-line fragments, being identified as rigid fragments and therefore increasing the abundance of light-cyan items. Finally, a particular resistance of the bluish colours to the UV radiation and associated nanofragmentation could also explain the observed patterns. However, we know little about the effects of additives on plastic photodecomposition, the colour-selectivity of visual active predators (Ryan 1987), or possible colour shifts of ingested plastic after with gut acid treatment. Consequently, no hypothesis can be ruled out yet in relation to the abundance of bluish plastics at sea.

Yellow and brown colours were also particularly abundant in our collection of marine plastic debris (Fig. 3). The phenomena of yellowing and tanning are commonly

observed in all of the most common plastic polymers, including PE, PP, PS, PET or PVC (Brandon et al. 2016, Andrady 2017). The degree of yellow or brown colour is associated with the amount of products resulting from the photo-oxidation, hence the extent of the weathering (Andrady 1997; ter Halle et al. 2016). The oxidative process may act on the polymer itself (e.g. PVC, PC, PS) as well as on the thermal stabilizers added to the plastic resin (Andrady 2017). The dependence of the yellow-brown colouration on the nature and concentration of additives in the plastic matrix (Cooper & Corcoran 2010; Fisner et al. 2017) makes the analyses based on these colours complex due to the plethora of additives in the market. However, our analysis provides a consistent pattern in the abundance of yellow and brown items across the plastic size gradient (Fig. 4B). Light yellow items reached the highest proportions in plastic items around 1 centimetre in size, while fragments around 1 millimetre tended to be light brown in colour (Fig. 4B). This pattern was consistent across independent datasets, from open-ocean and semi-enclosed seas, which renders this a robust result (Fig. S8). We must note this analysis focused on rigid floating fragments. As in other sea-surface datasets, only two low-density polymers (PP and PE) accounted for most of the fragments in our dataset (Serranti et al. 2018, Pedrotti et al. 2016), which must reduce the variability of yellowing and tanning patterns expected for the diversity of plastic resins in the market.

Interestingly, weathering testing with plastic materials suggests a typical progressive shift from white to yellow to brownish colour upon an extended solar exposure (Andrady 2017), matching with our finding of a succession of the peaks of yellow and brown items across the marine plastic size gradient. Combining colour and size distributions of marine plastic items provides a pathway to infer age for microplastic samples by using, for example, ratios of colours or RGB scores (Table S1). Indeed, the

322 combination of RGB scores into yellowing indexes is commonly used by the polymer
323 industry to assess the degradation of the plastic materials exposed to solar radiation (e.g.
324 Andrady 2017).

325 The experience acquired with the present work has allowed defining a systematic
326 method to the colour analysis based on a 120-colour palette as reference to assign
327 colours. The design of the reference palette (120-Palette) was optimized to provide an
328 operational method, in terms of observer's capacity and analytical effort, as well as a
329 thorough colour categorization able to be applied to other studies or purposes, including
330 unexplored sites with potentially different colour spectra or other applications that
331 cannot be anticipated. In this study, we simplified the colour scheme of the 120-Palette
332 for the statistical PCA analysis, due to the low representativeness of some colours in our
333 dataset. The samples might be processed, if needed, using a simplified reference palette
334 derived from the aggregation of dark, medium and light hues (42-Palette, see Methods).
335 However, working with a 120-Palette was not excessively demanding and the gathering
336 of additional information by using the 120-Palette would contribute to expand the
337 standardized high-detail colour dataset provided here (Table S3). The current baseline
338 dataset was fully obtained from the visual method. Based on this experience, we
339 developed a comparable alternative digital method to advance in the automatization of
340 the colour assessment if future analyses (see Supporting Methods).

341 In addition to providing tools and an empirical benchmark for analysing colours, here
342 we discussed about the processes controlling the colour distribution of the marine
343 plastic. Colour changes (whitening, yellowing and tanning) possibly related to the
344 photo-oxidative degradation were identified as main processes modulating the colour
345 spectrum of marine plastic. Our results provide a first evidence for a relationship
346 between distance to land, size and colour of marine plastic debris, suggesting that colour

may provide a qualitative proxy for the age of marine plastic samples, particularly when combined with size. White, yellow and brown colours, or a combination of them a priori appear as the most suitable colours to devise information about ageing. However, further and more focused research is required to assess whether colour and size distributions can be jointly used to provide a robust proxy of the age of plastics at sea.

ASSOCIATED CONTENT

Supporting information. Additional figures and tables.

AUTHOR INFORMATION

* Corresponding authors: elisa.marti@uca.es; andres.cozar@uca.es

Author Contributions

EM, FE, CD and AC conceived and designed the study; EM, CM and MG processed the samples; EM, FE, CD and AC contributed to analysis and interpretation of data; EM and AC drafted the manuscript and EM, CM, MG, FE, CD and AC reviewed the manuscript.

Conflict of Interest Statement

The authors declare no competing financial interest.

Acknowledgments

This study is an outcome of Malaspina 2010 expedition (Consolider-Ingenio 2010, CSD2008-00077). E.M. was supported by the Campus de Excelencia Internacional del Mar (CEIMAR) through a PhD Research Project Grant. We received additional support from PLASTREND (BBVA Foundation) and MIDaS (CTM2016- 77106-R,

AEI/FEDER/UE) projects. We thank personnel from Malaspina 2010 expedition, MEDSea (EU contract number FP7-2010-265103), TARA Arctic Ocean, MAFIA (*Migrants and Active Flux In the Atlantic Ocean*), MEGAN (*Mesoscale and submesoscale processes in the Strait of Gibraltar: The Trafalgar-Alborán connection*), Seagrass and Mangrove Cruise through Red Sea and ETO y NST Cruise along Bay of Biscay, for the help with the sample collection.

References

(1) Cózar, A.; Echevarría, F.; González-Gordillo, J. I.; Irigoien, X.; Úbeda, B.; Hernández-León, S.; Palma, A. T.; Navarro, S.; García-de-Lomas, J.; Ruiz, A.; et al. Plastic Debris in the Open Ocean. *Proc. Natl. Acad. Sci. U. S. A.* **2014**, *111* (28), 10239–10244. https://doi.org/10.1073/pnas.1314705111.

(2) Eriksen, M.; Lebreton, L. C. M.; Carson, H. S.; Thiel, M.; Moore, C. J.; Borerro, J. C.; Galgani, F.; Ryan, P. G.; Reisser, J. Plastic Pollution in the World's Oceans: More than 5 Trillion Plastic Pieces Weighing over 250,000 Tons Afloat at Sea. *PLoS One* **2014**, *9* (12), e111913. https://doi.org/10.1371/journal.pone.0111913.

(3) van Sebille, E.; Wilcox, C.; Lebreton, L.; Maximenko, N.; Hardesty, B. D.; van Franeker, J. A.; Eriksen, M.; Siegel, D.; Galgani, F.; Law, K. L. A Global Inventory of Small Floating Plastic Debris. *Environ. Res. Lett.* **2015**, *10* (12), 124006. https://doi.org/10.1088/1748-9326/10/12/124006.

(4) Brandon, J.; Goldstein, M.; Ohman, M. D. Long-Term Aging and Degradation of Microplastic Particles: Comparing in Situ Oceanic and Experimental Weathering Patterns. *Mar. Pollut. Bull.* **2016**, *110* (1), 299–308. https://doi.org/10.1016/j.marpolbul.2016.06.048.

(5) ter Halle, A.; Ladirat, L.; Martignac, M.; Mingotaud, A. F.; Boyron, O.; Perez, E.

393 To What Extent Are Microplastics from the Open Ocean Weathered? *Environ.*
394 *Pollut.* **2017**, *227*, 167–174. https://doi.org/10.1016/j.envpol.2017.04.051.
395 (6) Zhang, H. Transport of Microplastics in Coastal Seas. *Estuar. Coast. Shelf Sci.*
396 **2017**, *199*, 74–86. https://doi.org/10.1016/j.ecss.2017.09.032.
397 (7) Cózar, A.; Martí, E.; Duarte, C. M.; García-de-lomas, J.; Sebille, E. Van;
398 Ballatore, T. J.; Eguíluz, V. M.; González-Gordillo, J. I.; Pedrotti, M. L.;
399 Echevarría, F.; Troublè, R.; Irigoien, X. The Arctic Ocean as a Dead End for
400 Floating Plastics in the North Atlantic Branch of the Thermohaline Circulation.
401 *Sci. Adv.* **2017**, *3*, 1–8.
402 (8) Weinstein, J. E.; Crocker, B. K.; Gray, A. D. From Macroplastic to Microplastic:
403 Degradation of High-Density Polyethylene, Polypropylene, and Polystyrene in a
404 Salt Marsh Habitat. *Environ. Toxicol. Chem.* **2016**, *35* (7), 1632–1640.
405 https://doi.org/10.1002/etc.3432.
406 (9) ter Halle, A.; Ladirat, L.; Gendre, X.; Goudounèche, D.; Pusineri, C.; Routaboul,
407 C.; Tenailleau, C.; Duployer, B.; Perez, E. Understanding the Fragmentation
408 Pattern of Marine Plastic Debris. *Environ. Sci. Technol.* **2016**, *50*, 5668–5675.
409 https://doi.org/10.1021/acs.est.6b00594.
410 (10) Pospísil, J.; Nespurek, S.; Zweifel, H.; Kuthan, J. Photo-Bleaching of Polymer
411 Discoloration Caused by Quinone Methides. *Polym. Degrad. Stab.* **2002**, *78*,
412 251–255.
413 (11) Andrady, A. L.; Searle, N. D.; Crewdson, L. F. E. Wavelength Sensitivity of
414 Unstabilized and UV Stabilized Polycarbonate to Solar Simulated Radiation.
415 *Polym. Degrad. Stab.* **1992**, *35* (3), 235–247. https://doi.org/10.1016/0141-
416 3910(92)90031-Y.
417 (12) Singh, R. P.; Tomer, N. S.; Bhadraiah, S. V. Photo-Oxidation Studies on

418 Polyurethane Coating: Effect of Additives on Yellowing of Polyurethane. *Polym.*
419 *Degrad. Stab.* **2001**, *73* (3), 443–446. https://doi.org/10.1016/S0141-
420 3910(01)00127-6.
421 (13) Yousif, E.; Haddad, R. Photodegradation and Photostabilization of Polymers,
422 Especially Polystyrene: Review. *Springerplus* **2013**, *2* (1), 398.
423 https://doi.org/10.1186/2193-1801-2-398.
424 (14) Pastorelli, G.; Cucci, C.; Garcia, O.; Piantanida, G.; Elnaggar, A.; Cassar, M.;
425 Strlič, M. Environmentally Induced Colour Change during Natural Degradation
426 of Selected Polymers. *Polym. Degrad. Stab.* **2014**, *107*, 198–209.
427 https://doi.org/10.1016/j.polymdegradstab.2013.11.007.
428 (15) Shaw, D. G.; Day, R. H. Colour- and Form-Dependent Loss of Plastic Micro-
429 Debris from the North Pacific Ocean. *Mar. Pollut. Bull.* **1994**, *28* (1), 39–43.
430 https://doi.org/10.1016/0025-326X(94)90184-8.
431 (16) Barrows, A. P. W.; Neumann, C. A.; Berger, M. L.; Shaw, S. D. Grab vs.
432 Neuston Tow Net: A Microplastic Sampling Performance Comparison and
433 Possible Advances in the Field. *Anal. Methods* **2017**, *9*, 1–8.
434 https://doi.org/10.1039/C6AY02387H.
435 (17) Blair Crawford, C.; Quinn, B. *Microplastic Pollutants 2017*; 2017.
436 (18) Hartmann, N. B.; Hüffer, T.; Thompson, R. C.; Hassellöv, M.; Verschoor, A.;
437 Daugaard, A. E.; Rist, S.; Karlsson, T.; Brennholt, N.; Cole, M.; Herrling, M. P.;
438 Hess, M. C.; Ivleva, N. P.; Lusher, A. L.; Wagner, M. Are We Speaking the
439 Same Language? Recommendations for a Definition and Categorization
440 Framework for Plastic Debris. Environ. Sci. Technol. 2019, 53, 1039–1047.
441 (19) Andrady, A. L. The Plastic in Microplastics: A Review. Mar. Pollut. Bull. 2017.
442 https://doi.org/10.1016/j.marpolbul.2017.01.082.

443 (20) Serranti, S.; Palmieri, R.; Bonifazi, G.; Cózar, A. Characterization of
444 Microplastic Litter from Oceans by an Innovative Approach Based on
445 Hyperspectral Imaging. *Waste Manag.* **2018**.
446 https://doi.org/10.1016/j.wasman.2018.03.003.
447 (21) Cózar, A.; Sanz-Martín, M.; Martí, E.; González-Gordillo, J. I.; Úbeda, B.;
448 Gálvez, J. Á.; Irigoien, X.; Duarte, C. M. Plastic Accumulation in the
449 Mediterranean Sea. *PLoS One* **2015**, *10* (4), e0121762.
450 https://doi.org/10.1371/journal.pone.0121762.
451 (22) Martí, E.; Martin, C.; Cózar, A.; Duarte, C. M. Low Abundance of Plastic
452 Fragments in the Surface Waters of the Red Sea. *Front. Mar. Sci.* **2017**, *4* (333),
453 1–8. https://doi.org/10.3389/fmars.2017.00333.
454 (23) Morét-Ferguson, S. E.; Law, K. L.; Proskurowski, G.; Murphy, E. K.; Peacock,
455 E. E.; Reddy, C. M. The Size, Mass, and Composition of Plastic Debris in the
456 Western North Atlantic Ocean. *Mar. Pollut. Bull.* **2010**, *60* (10), 1873–1878.
457 https://doi.org/10.1016/j.marpolbul.2010.07.020.
458 (24) Reisser, J.; Slat, B.; Noble, K.; du Plessis, K.; Epp, M.; Proietti, M.; de
459 Sonneville, J.; Becker, T.; Pattiaratchi, C. The Vertical Distribution of Buoyant
460 Plastics at Sea: An Observational Study in the North Atlantic Gyre.
461 *Biogeosciences* **2015**, *12* (4), 1249–1256. https://doi.org/10.5194/bg-12-1249-
462 2015.
463 (25) Hudelson, K. Ultraviolet Radiation Tolerance in High Elevation Copepods from
464 Ultraviolet Radiation Tolerance in High Elevation Copepods from the Rocky
465 Mountains of Colorado, USA., **2011**.
466 (26) Umbers, K. D. L. On the Perception, Production and Function of Blue
467 Colouration in Animals. *J. Zool.* **2012**, *289*, 229–242.

https://doi.org/10.1111/jzo.12001.

(27) Ory, N. C.; Sobral, P.; Ferreira, J. L.; Thiel, M. Amberstripe Scad Decapterus Muroadsi (Carangidae) Fish Ingest Blue Microplastics Resembling Their Copepod Prey along the Coast of Rapa Nui (Easter Island) in the South Pacific Subtropical Gyre. Sci. Total Environ. **2017**, 586, 430–437. https://doi.org/10.1016/j.scitotenv.2017.01.175.

(28) Ryan, P. G. The Incidence and Characteristics of Plastic Particles Ingested by Seabirds. *Mar. Environ. Res.* **1987**, *23* (3), 175–206. https://doi.org/10.1016/0141-1136(87)90028-6.

(29) Andrady, A. L. Wavelength Sensitivity in Polymer Photodegradation. In Advances in Polymer Science; 1997; Vol. 128, pp 47–94. https://doi.org/10.1007/3-540-61218-1_6.

(30) Cooper, D. A.; Corcoran, P. L. Effects of Mechanical and Chemical Processes on the Degradation of Plastic Beach Debris on the Island of Kauai, Hawaii. *Mar. Pollut. Bull.* **2010**, *60* (5), 650–654. https://doi.org/10.1016/j.marpolbul.2009.12.026.

(31) Fisner, M.; Majer, A.; Taniguchi, S.; Bícego, M.; Turra, A.; Gorman, D. Colour Spectrum and Resin-Type Determine the Concentration and Composition of Polycyclic Aromatic Hydrocarbons (PAHs) in Plastic Pellets. *Mar. Pollut. Bull.* **2017**, *122* (1–2), 323–330. https://doi.org/10.1016/j.marpolbul.2017.06.072.

(32) Pedrotti, M. L.; Petit, S.; Elineau, A.; Bruzaud, S.; Crebassa, J.-C.; Dumontet, B.; Martí, E.; Gorsky, G.; Cózar, A. Changes in the Floating Plastic Pollution of the Mediterranean Sea in Relation to the Distance to Land. *PLoS One* **2016**, *11* (8), e0161581. https://doi.org/10.1371/journal.pone.0161581.

493

494